ChemComm

Cite this: *Chem. Commun.*, 2011, **47**, 9972–9985

www.rsc.org/chemcomm

FEATURE ARTICLE

Mesoporous silica nanoparticles as nanocarriers

Si-Han Wu, Yann Hung and Chung-Yuan Mou*

Received 28th March 2011, Accepted 24th May 2011
DOI: 10.1039/c1cc11760b

Modern nanomedicine aims at delivering drugs or cells specifically to defective cells; therefore, this calls for developing multifunctional nanocarriers for drug delivery and cell-tracking. Mesoporous silica nanoparticles (MSNs) are well suited for this task. In this feature article, we highlight the strategies in the synthesis and functionalization of small, uniform and colloidal stable MSNs. We then discuss cell uptake of MSNs and tracking cells, as both aspects are closely related to the efficacy of drug delivery and theranostics. Some examples of stimulated drug delivery are described. For application considerations, toxicity and pharmacokinetics are critical issues and *in vivo* studies are summarized.

Introduction

In the past decade, great strides have been made in nanomedicine, thanks to the rapid developments in nanomaterials.[1] In many developments of nanomedicine, various types of nanoparticles have been explored as drug carriers, diagnostic sensors, imaging probes, or labelling beacons. Many colloidal nanoparticles are engineered for cellular biology and biomedical applications. In the size range of 3 nm to a few hundred nanometres, a wide variety of materials—including metals, oxides, carbon materials and semiconductors—exhibiting unique optical,[2] magnetic[3,4] and chemical[5] properties have been developed. A clever combination of various modalities to build a multifunctional platform on nanoparticles for theranostic goals that afford both diagnostic and therapeutic capabilities is much desired. Mesoporous silica nanoparticles (MSNs), whose attributes include uniform mesopores, easy functionalization and significant biocompatibility, have gained much recent attention for biomedical applications.[6–8] The pore compartments and large surface area provide a natural platform for building a multifunctional theranostic agent. The unique topology provides MSNs with three distinct domains that can be independently functionalized: the silica framework, the nanochannels/pores, and the nanoparticle's outermost surface. As such, MSNs are especially well-suited to the task of incorporating the essential capabilities of a theranostic

Department of Chemistry, National Taiwan University, No. 1, Sec. 4, Roosevelt Road, Taipei, Taiwan 10617. E-mail: cymou@ntu.edu.tw; Fax: +886-2-23660954

Si-Han Wu, Yann Hung and Chung-Yuan Mou

Si-Han Wu was born in 1982 in Taiwan. He received his BS degree in Chemistry from Fu-Jen Catholic University, followed by his MS degree from National Taiwan University in 2007. He is currently pursuing his PhD degree under the supervision of Prof. Chung-Yuan Mou at the National Taiwan University. His research interests are in the field of biomaterials, focusing on the build-up of theranostic nanocarriers.

Yann Hung received her BS from National Taiwan University and PhD in Inorganic Chemistry from the Ohio State University. Currently, she is a research associate in Prof. Mou's group. She has worked on a variety of research projects including photocopier related issues, surface characterization of hard disks, etc. Her research interests are materials oriented, aiming at the biological applications.

Chung-Yuan Mou received his BS from National Taiwan University and earned his PhD in Theoretical Chemistry from Washington University in St. Louis. After postdoctoral researches, he joined National Taiwan University in 1978 where he is now the University Chair Professor of Chemistry. He has been awarded the National Chair Professor (2000), the Chinese Chemical Society Metal (2002), and the Cozarrelli Prize of PNAS (2007). His research interests include biomedical applications of mesoporous silica, heterogeneous catalysis, supercooled water, confined enzymes and biomineralization.

platform in a single particle, with separate domains for (1) the contrast agent that enables traceable imaging of theranostic target, (2) the drug payload for therapeutic intervention, and (3) the biomolecular ligand for highly targeted delivery. In addition to these attributes, MSNs have been demonstrated to show *in vivo* biocompatibility,[9] straightforward surface functionalization,[10] and avid cell uptake.[11]

Many possible modalities on MSNs are available for theranostic applications. The interior pores can protect a high loading of organic molecules such as fluorescent or MRI contrast agents. The external surface can be selectively functionalized to give site-specific targeting ability such that various strategies for intracellular delivery can be realized.[12] Pores can be containers for drugs, DNA or RNA to be delivered.[13,14] MSNs can also be used for the immobilization of functional enzymes.[15] Here in this feature article, we review recent research towards biomedical applications of MSNs, particularly the works from our laboratory. For the general purpose of building various functionalities on MSNs, methods of synthesizing and functionalization of MSNs are critically reviewed. Our understanding on the cell uptake of MSNs is then discussed. Biomedical applications including imaging modalities, cell tracking and drug delivery are highlighted. Finally, we also review the biodistribution and toxicity of the MSNs.

Synthesis of mesoporous silica nanoparticles

For biomedical applications, synthetic strategies need to satisfy two conditions: (1) well-controlled nucleation and growth rate of MSNs to produce uniform sizes in the range of 30–300 nm, and (2) non-stickiness of the MSNs during work-up. In the early days of developing synthesis, many strategies were used to synthesize nanosized mesoporous silicas, including the use of different co-solvents, bases, surfactants, polymer protection and so on. Grün *et al.* first modified the Stőber synthesis of monodisperse silica spheres by adding a cationic surfactant to the reaction mixture and obtained submicrometer-scaled MCM-41 particles.[16] Cai *et al.* and Nooney *et al.* found a very dilute condition of surfactant is crucial for obtaining MCM-41 silicas of size $\sim$100 nm.[17,18] Imai and co-workers obtained mesostructured silica nanoparticles with size below 50 nm using a double surfactant system.[19] Ying and co-workers used a mixture of fluorocarbon and hydrocarbon surfactants to synthesize IBN mesoporous silica with some size control in the several hundred nm range.[20] Urata *et al.* utilized a dialysis process to remove surfactants as well as prevent aggregation of MSNs with diameter less than 20 nm.[21] In recent years, to satisfy biomedical applications, the synthesis of MSNs demands tighter control of size and suspension stability. Using phosphate buffer solution as the reaction medium, He *et al.* successfully synthesized uniform MSNs (40–600 nm) by tuning the temperature, structure-directing agent, co-surfactant and co-solvent.[22] In the synthesis, one must consider the nucleation, growth and aggregation processes driven by the silica condensation reaction. In a well-controlled process, one would like to have a short burst of nucleation and uniform growth while avoiding any aggregation. Thus, alkaline and highly diluted conditions are usually used to lead to a negatively charged and more fully condensed surface, to avoid inter-particle aggregations.

In most of the syntheses of MSNs, cationic cetyltrimethylammonium surfactants are employed owing to their strong association with silica precursors. SBA-15 is much more difficult to reduce to nano-size due to its acidic synthetic conditions. The resulting particles are either sticky rods with length more than 400 nm[23] or poor in size distribution.[24] Shi and co-workers recently reported the morphologies and dimensions of SBA-15-type MSNs can be tailored by incorporation of multivalent metal salts,[25] however, the size and polydispersity of particles still cannot adequately meet the demands for most biological applications. Thus, in the following, we discuss only the synthetic control of MSNs based on cetyltrimethylammonium surfactants. Broadly speaking, there are three approaches of morphology control in the 100 nanometre size range.

(a) Growth–quench approach

Mann and co-workers[26] first used a dilution and pH change method to quench the silica condensation reaction to obtain sub-100 nm mesoporous silica nanoparticles. Using different time-delay between dilution and neutralization steps, the particle size of the materials could vary from 23 to 100 nm. Other reaction-slowing agents have since been used, such as triethanolamine[27] and alcohol co-solvents[28] for their silicon-chelating ability. However, due to the poor condensation of silica, the resulting MSN materials from pH quench are often less ordered and less stable in solution. Moreover in the dilution quench approach, one may have the problem of scaling up. For avoiding an excess amount of water, the polyalcohol base triethanolamine as a substitute for commonly used NaOH or NH_3 (aq) may be employed. Recently, Suteewong *et al.*[29] synthesized MSNs of cubic pore structure with highly aminated functionality in which ethyl acetate was used to quench the growth.

(b) Confinement approach

If synthesis of MSNs is done in a confined media, the particle size can be limited. An aerosol-assisted self assembly of mesoporous spherical nanoparticles has been developed by Brinker and co-workers.[30] The method relies on evaporation-induced interfacial self-assembly confined to spherical aerosol droplets. However, the method is not widely adopted because of the need of equipment for aerosol production.

Just like in the solution syntheses of metallic or semiconductor nanoparticles, encapsulation agents can be used to keep the MSNs from growing to micron-size. Polyethylene glycol[28,31] has been introduced to reduce the particle size of MSNs. Recently, F127 has been used as a dispersion agent to synthesize MSNs.[32,33] With increasing amount of F127, the average particle size of MSNs is decreased.

A recent trend is to synthesize hollow nanospheres with a mesoporous silica shell. An advantage of hollow form of MSNs is its interior space can be used as a container for other cargo, such as magnetic,[34] gold or silica[35] nanoparticles. Soft templates, such as vesicles, microemulsions and micelles may be used to condense silica to create the hollow nanospheres. Niu *et al.* synthesized core–shell structured dual-mesoporous silica spheres (DMSS) with smaller pores (2.0 nm) in the shell and larger tunable pores in the core.[36] Early on, Yeh *et al.*

created hollow silica spheres with mesostructured shells with a vesicle template of mixed surfactant system of CTAB-SDS–Pluronic 123, in which a vesicle structure was made from the catanionic surfactants CTAB/SDS.[37] Other catanionic type vesicles have been reported for making hollow nanospheres of silica.[38] Alternatively the vesicle structure may be assisted by ultrasound.[39] More recently, complicated hollow silica structures are appearing: chiral mesoporous organosilica nanospheres with uniform particle size were created for catalytic asymmetric reaction.[40] Multi-shelled mesoporous silica hollow nanospheres have also been templated from vesicles[35,41] or can be built as rattle-type or hollow structures in a shell-by-shell approach.[42] Chen *et al.* took an etching approach to create uniform hollow inorganic core/shell structured multifunctional mesoporous nanocapsules.[43]

A different confinement strategy is to use a microemulsion in the synthesis of MSNs.[44,45] Because a microemulsion is a thermodynamic equilibrium system, its phase domain is rather uniform in size. Mou and co-workers used a microemulsion system to confine the synthesis of MSNs to prepare rather uniformly sized silica nanoparticles either in hollow or solid form.[44] A water/heptane/CTAB nanoemulsion induced by compressed CO_2 was used to make hollow spherical MSNs.[45] More recently, silica-coated[46] or organosilica-coated[47] block-copolymer (F127) micelles were used to create ultra-small uniform sizes of $\sim$25 nm of hollow porous nanospheres.

(c) Separation of nucleation and growth

Mou and co-workers developed a method of synthesizing mono-disperse MSNs by separating the nuclei formation and particle growth into two steps in a dilute alkaline solution.[48] The method can be understood in a LaMer diagram of concentration change during nucleation and growth. In the first step (step (A) in Fig. 1), the full amount of surfactant (CTAB) and a small amount of TEOS are mixed to form a clear solution of micelle/silicate clusters containing nuclei. Then, a larger amount of TEOS is added to start the growth process without further nucleation (step (B) in Fig. 1). Finally, with the growth process accelerating, the materials are exhausted resulting in a uniform finite size. The MSN materials thus obtained possess excellent structure order, showing four XRD peaks for a 100 nm size MSN. Often, MSNs show hexagonal facets, meaning no aggregation occurred. We later demonstrated that the particle size of MSNs can be modulated by controlling the pH of the reaction solution.[49] A decrease in particle size from 280 to 30 nm can be observed accompanying the reduction of the amount of ammonia. At lower pH, there are larger numbers of nuclei, therefore resulting in smaller MSN particles. The method seems to be size-focusing,[50] giving very sharp distribution of size and shape. In fact, in an optimized synthesis condition, Lin *et al.* could obtain regular hexagons which are so regular in size that a 2D photonic crystal-like structure could be self-assembled from them.[51]

Surface functionalization of mesoporous silica nanoparticles

MSNs possess well-defined structure and high density of surface silanol groups which can be modified with a wide range of organic functional groups.[52] The surface functional groups can play several roles in biomedical applications of MSNs: (i) to control the surface charge of MSNs; (ii) to chemically link with functional molecules inside or outside the pores; and (iii) to control the size of pore entrance for entrapping molecules in the nanopores.

There are three methods of surface functionalization for MSNs: co-condensation, post-synthesis grafting and surfactant displacement methods. In the one-pot co-condensation process, organosilanes are added directly in the synthesizing gel solution together with a silica source.[53] Then, the surfactant molecules can be removed by ion exchange with an ethanolic solution of ammonium nitrate[54] or HCl.[53,55] The advantages of co-condensation are a simple operation, uniformity in distribution of functionalization, and achievable high loading. However, under some conditions, the extraction of surfactants may not be complete, depending on the solvent. In the grafting method, one introduces the functional groups after removal of the templates, by calcination or extraction.[56] This method offers many possibilities for functional group placements allowing the

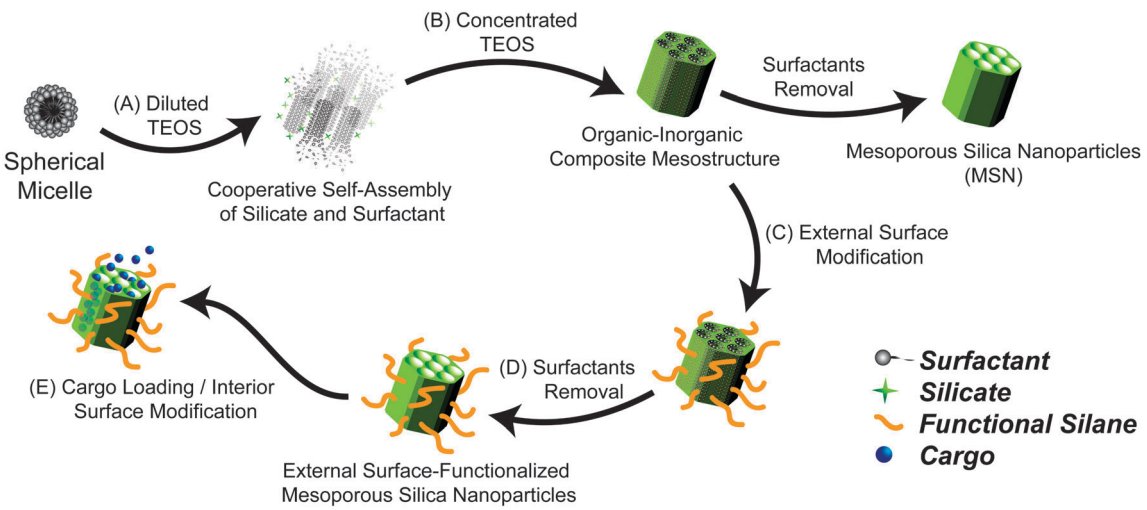

Fig. 1 Schematic illustration for the synthesis and selective functionalization of MSNs.

grafting of chemically more delicate organic functionalities prone to hydrolysis and elimination reactions.[57] However, the distribution of functional groups may not be uniform if the blocking of nanopores occurs.[58] A combination of co-condensation and grafting method has been used to create a bi-functional surface modification of mesoporous silica.[59] In an extension of the grafting method, Mou's laboratory reported a direct surface silylation with simultaneous surfactant extraction without prior calcination, by using acidic alcohol as the solvent.[60,61] Because of the weaker $S^+X^-I^+$ interaction in acidic conditions, surfactants can be removed by proton exchange and solvent extraction. This surfactant displacement method produces a uniform monolayer coverage with precisely controllable amounts of functionalized organosilanes on the surface.

There have been a large number of reports on the surface functionalization of mesoporous silica. For a recent review, please see Brühwiler.[10] However, we choose to review two topics which are particularly important for the biomedical applications of MSNs: charge control and selective functionalization.

(a) Functionalization for charge control

It is known that the cell internalization of nanocarriers is strongly influenced by the physicochemical properties of the nanoparticles, of which surface charge is one of the deciding factors.[62] With a large internal and external surface, the surface potential of MSNs can be precisely controlled by the functionalization of charged chemical groups. For many applications, amine functional groups such as 3-aminopropyltrialkoxysilane (APTS) are often used, giving a positive charge due to protonation in a pH-dependent manner.[63] Due to the negatively charged character of the cell plasma membrane, nanocarriers possessing a positively charged surface generally display better association and up-take rates.[64] For strongly positively charged MSNs, quaternary ammonium end groups such as *N*-trimethoxysilylpropyl-*N*,*N*,*N*-trimethylammonium (TA) may be used.[11] On the other hand, unmodified MSNs are normally negatively charged at neutral pH. He *et al.* found much less cell uptake of calcined MSNs as they are negatively charged.[65] However, this could also be due to aggregation after calcination. For improving suspension stability of MSNs in solutions to carry hydrophobic drugs, Lu *et al.* have modified the surface of MSNs with phosphonate groups to carry a high negative charge.[66] Recently, anionic–cationic pH-switchable MSNs have been synthesized by dual amino and carboxylic acid functionalization.[67]

(b) Selective functionalization

Selective functionalization of the inner and outer surfaces of MSNs with different trialkoxysilanes offers different functionalities at different sites.[10] This is useful in a situation where a cell-recognition ligand is desired at the outer surface, while the internal surface is used for a second functionality. Conjugation of MSNs with two different alkoxysilanes can be performed through a two-step surface modification as shown in Fig. 1. The as-synthesized MSNs with surfactant still inside the pores may be first modified with one silane without removing the surfactant (step (C) in Fig. 1). The alkoxysilane would be grafted only onto the outer surface of the MSNs, while the inner surface is still available for the second graft after the templates are removed by acidic ethanol extraction (step (D) in Fig. 1). The functionalization of the inner surface (step (E) in Fig. 1) can also be done in either the co-condensation or surfactant displacement methods. The selective functionalization of the external surface is important in labelling the nanoparticles with specific groups for tumor cell targeting,[68] attaching molecules for pore gating[69] or creating high positive charge on the outer surface. Linden and co-workers realized preferential growth of hyperbranched poly(ethyleneimine), PEI, on the outer surface of the material which was achieved by growing the polymer before the surfactant extraction.[70] However, spatial selectivity in the two-step approach may not be very effective with MSNs in an alcohol solution, because template-filled MSNs still permit some diffusion of grafting agents into the mesopores. Bein and co-workers developed a multi-step co-condensation strategy such that better selective functionalization of the inner and outer surfaces of MSNs results in bifunctional nanoparticles.[71]

In fabricating multifunctional MSNs, one should pay special attention to the suspension stability of the MSN colloid. Often, after extensive surface modifications, the colloidal solution is no longer stable. Hence the hydrodynamic size of the MSNs needs to be checked repeatedly to make sure there is no serious aggregation of the nanoparticles in the solution.

Cell uptake

The first step towards understanding the response of biological cells to nanomaterials is to examine the cell uptake of the nanoparticles and their intracellular trafficking.[12] Fluorescence microscopy, in its various modern inventions, is primarily used for tracking the uptake and trafficking of the nanoparticles, provided they are labelled with appropriate chromophores or are intrinsically luminescent. With easy functionalization of the surface, MSNs can be labelled with various fluorescent agents such as the green emitting FITC,[48] or near-infrared (NIR) dye.[72] The later would be useful for *in vivo* real time imaging of animals due to the better penetration depth of NIR light. The semi-isolated pores lessen self-quenching and stabilize the chromophores. Other techniques for determining the cellular uptake are flow cytometry, transmission electron microscopy (TEM), and magnetic resonance imaging (MRI).

Cell uptake of nanoparticles depends on cell-type,[73,74] surface charge,[11,63] particle size,[49,74–79] particle shape,[80] and surface chemistry.[63,81] Furthermore, it is dosage and time dependent. One of the goals in studying nanoparticle-based delivery and cell-labelling agents is to correlate cell uptake with physicochemical properties of the engineered nanoparticles. MSNs are useful because their physicochemical properties are often quite well-characterized. With its extensive silica pore system and easy functionalization, labelling with fluorescence or MRI contrast agent is simple and one can follow the cell's response easily upon entry of the MSNs. Mou's laboratory studied in detail cell uptake of uniform 110 nm FITC-MSN which displays well-ordered channels, large surface area, and uniform pores. In addition, it suspends well in water, which is important for biological applications. Embedding FITC in MSNs has an advantage of improved photostability.[48] Cell uptake of FITC-MSN by human mesenchymal stem cells (hMSC) and

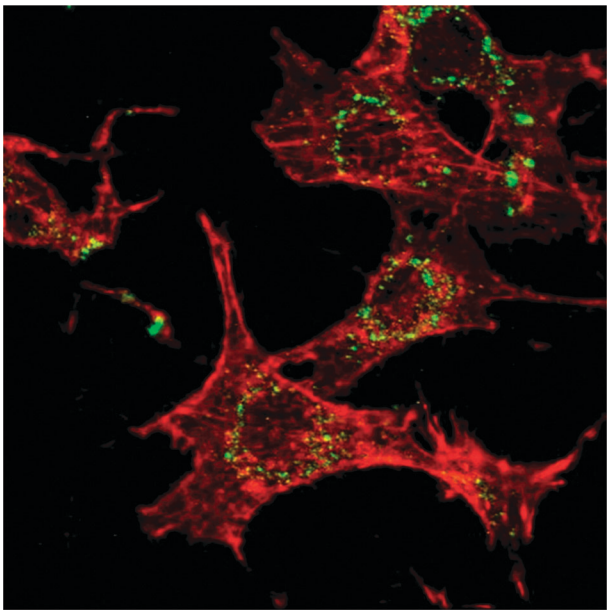

Fig. 2 Confocal images of FITC-MSNs (green) in 3T3-L1 cells; the cell skeleton was stained with rhodamine phalloidin (red). Cells were incubated with FITC-MSNs for 1 h, washed, and further incubated in particle-free medium overnight. (Reproduced with permission from ref. 48. Copyright 2005, American Chemical Society).

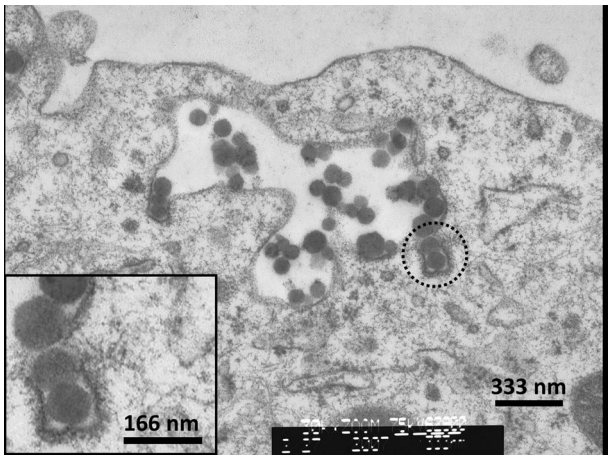

Fig. 3 TEM images of Her-Dye@MSN-1 internalized into BT-474. The image is near the cell surface during the uptake process. Inset is the high-resolution image of the area circled by a dashed line showing endocytosis involving a clathrin-like coated pit. (Reproduced with permission from ref. 68. Copyright 2009, Royal Society of Chemistry).

fibroblast cells were highly efficient. The nanoparticles did not penetrate the nuclear membrane (Fig. 2); instead they gathered around the perinuclear region of the cell. The internalized amount and residence time are cell-type dependent. Seven days after incubation, the nanoparticles were still present inside the hMSC while a diminished amount was shown in 3T3-L1 even at day 3.[48] Detailed endocytosis mechanism[82] of MSNs may be examined using various blocking agents.[73] For example, Huang *et al.* showed that clathrin-mediated endocytosis plays an important role in the uptake of nanoparticles in hMSCs, as the uptake was reduced with sucrose-induced hypertonicity, which inhibits the recruitment of clathrin.[73] Later, Tsai *et al.* used TEM imaging (Fig. 3) to show clearly the formation of clathrin pits in the engulfment of MSNs.[68]

One of the special characteristics of MSNs compared to other types of nanoparticles is their mesoporosity. Their surface is not smooth as in a solid particle but rather there are a lot of pore openings.

The interaction of MSNs with biological cells is of interest. It has been reported that the cell–substrate interaction depends on the dimensions of the underlying topography.[83] Even a small topographical change in nanoscale has been shown to cause specific cellular responses.[84] It is also reported that polymer membrane porosity in the size range of 6–12 nm influences the initial cell–surface interactions, and increasing pore size augmented cell adhesion and aggregate formation.[85] Liu *et al.*[86] first showed that mesoporosity improved cell uptake of MSNs labelled with magnetic iron oxide as compared to solid silica nanoparticles. Furthermore, Lin's laboratory reported MSNs show better biocompatibility compared to silica nanoparticles.[87]

The problem of the size effect on cell uptake of nanoparticles is a currently important issue in the field of nanobiology. Particle size is an important parameter in designing suitable cell-tracking and drug-carrier nanoparticle systems. The two-step synthetic method developed by Mou's laboratory gives sharply defined sizes of MSNs depending on pH. Uptake studies of a series of MSNs from 30 to 280 nm into HeLa cells revealed that 50 nm MSNs enter cells most efficiently.[49] It is interesting to note that for particles that enter cells through clathrin-mediated endocytosis, 50 nm nanoparticles appear to be the most efficient ones for various materials.[76–79] Chithrani and Chan proposed that the wrapping time, which is affected by the adhesion, membrane stretching and bending energy of membrane, as well as the receptor diffusion, are the two competing factors affecting the uptake.[77] Thus, unfavorable free energy of the interaction impairs uptake of small nanoparticles, whereas slower receptor diffusion causes less uptake of large nanoparticles. Caveolae-mediated endocytosis has also been reported for differently functionalized MSNs (150 nm).[63] Studies using polystyrene of different sizes showed the uptake mechanism is also size dependent, *i.e. via* clathrin-coated pits for diameter smaller than 200 nm and caveolae-mediated internalization for size 500 nm.[75] However, this does not hold for all nanoparticles.[11,63]

The kinetics of uptake and exocytosis of transferrin-coated nanogold (through clathrin-mediated endocytosis) of different sizes and shapes have been studied in three non-phagocytic cells, STO, HeLa and SNB19 cells.[77] The half-lives for exocytosis are much faster than that of endocytosis, and small nanoparticles exocytose faster. No detailed studies on the exocytosis of MSNs have been reported. One should be aware that for some cells, exocytosis of nanoparticles may be so effective that the time window for intra-cellular drug delivery may be rather limited.

It is well known that cell uptake is influenced by the surface chemistry of the nanoparticles. If the surface group is ionizable, MSNs would be highly charged. The extent of charge can be precisely controlled by the density of surface functionalization. Chung *et al.*[11] demonstrated the charge effect of cell-uptake of MSNs with varying grafted quaternary ammonium groups. At low surface charge, the normal clathrin- and actin-dependent mechanisms operate, which are already quite efficient for hMSC

and 3T3-L1 cells. Above a certain threshold of surface charge, a new charge-dependent mechanism, likely to be direct penetration, starts to be effective.[11]

In order to prevent nonspecific cell uptake, polyethylene glycol (PEG) is widely used.[88] Since FITC-MSN can be internalized non-specifically, it is necessary to diminish this unwanted process when cell-targeting is desired. Targeted drug delivery has many advantages such as reducing the damage to healthy tissues and more efficient disease treatment. Usually, the carrier surface is modified with targeting ligands to recognize the target. Small molecules have been attached to MSNs to demonstrate targeting. For example, folic acid has been widely used for this purpose.[63,89] However, folic acid was grafted after the surfactant was removed, raising the possibility that most of the folic acids were in the internal surface area. Mannosylated polyethylenimine has been exploited for targeting macrophage cells with mannose receptors.[90]

In a targeting design reported by Mou and co-workers, a potent cell-recognition agent, a monoclonal antibody (mAb)-Herceptin, was conjugated to the surface of the FITC-MSN, resulting in modified surface characteristics to target Her2/neu glycoprotein, which is a member of epidermal growth factor receptors. The FITC-MSN targeting platform includes a monoclonal antibody, Herceptin, a PEG linker to avoid nonspecific binding, and –SH derivatized FITC-MSN, as shown in Fig. 4.

The external surface of FITC-MSN was grafted with mercaptopropylsilane which is then conjugated with Herceptin-PEG-Mal through the SH group forming a targeted carrier, Her-Dye@MSN.[68] The targeting specificity of the platform was demonstrated using NIH3T3, MCF-7 and BT-474 cells. Of these, only BT-474 over-expresses Her/neu glycoprotein. It was found that nanoparticles with high amount of Herceptin showed much greater selectivity towards BT-474. TEM and competition studies of the internalization of Her-Dye@MSN undoubtedly manifested the uptake was through receptor-mediated endocytosis.[68] Zhu *et al*. have recently used a cancer cell-specific DNA aptamer as the targeting recognition agent to conjugate on MSNs.[91] They found good specificity in targeted delivery.

In a novel approach, Brinker and co-workers coated MSNs with lipid bilayers to create so-called protocells.[92] The name reflects the cell membrane-like behaviour of the bilayer on which existing surface functionalization of the liposome can be used. This has a great advantage because the targeting peptides anchored in the lipid bilayers are fluidic, multivalency

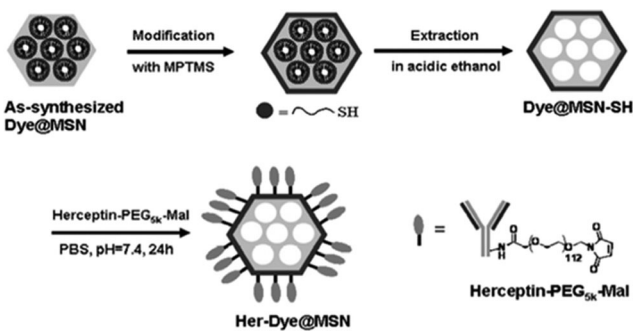

Fig. 4 Conjugation of Dye@MSN with Herceptin through a multi-step modification. (Reproduced with permission from ref. 68. Copyright 2009, Royal Society of Chemistry).

effect can be accomplished without a very high level of surface coverage of targeting agents. Their SP94 functionalized protocells exhibit a 10 000-fold greater affinity for human hepatocellular carcinoma than for hepatocytes, endothelial cells or immune cells.

After cell-uptake, MSNs would be usually trapped in the endosome. Hence some endosomal escape mechanism built into the nanoparticles would be quite useful for drug delivery applications. One method is to immobilize a proton sponge on the nanoparticle such that osmotic influx upon protonation of the sponge base can break the endosome.[93] A standard approach is to immobilize polyamines such as polyethyleneimine (PEI) onto the nanoparticle.[94] Huang *et al*. first noticed that the amine-functionalized FITC-MSN could serve as a proton sponge and help the endosome escape.[73] On delivering FITC-MSN to human mesenchymal stem cells (hMSC), partial co-localization of LysoTracker Red (red fluorescence) with the green FITC-MSN and some co-localization with nonyl-acridine orange (a mitochondria-selective probe) separately imply that FITC-MSN can escape endocytic vesicles.[73] This is because FITC-MSN contains many surplus amine groups (APTS for attaching FITC) which was protonated in the acidic environment of endosome, and the nanoparticles escaped to the cytosol.

Another approach for engineering endosome escape is by photochemical triggering of a photosensitizer attached to MSNs.[95] Sauer *et al*.,[96] by using Bein's selective functionalization method, built a photo-triggered endosome escape for release of MSN-encapsulated small molecules to the cytosol *via* redox-driven cleavage of disulfide bonds.

Magnetic resonance imaging

The capability of tracking the biodistributions of nanoparticles and their cargos in cell or *in vivo* is critical in the use of nanoparticles for drug and gene delivery.[97] Although fluorescence imaging could be achieved in *in vivo* monitoring with near infrared excitation, the penetration depth is limited. In order to monitor the nanocarrier *in vivo*, magnetic resonance imaging (MRI) is widely considered as a great technique because of its noninvasive nature. It would be of great advantage to combine optical (for pathological information) and MR imaging. However, MRI suffers low sensitivity for cell labelling.[98] Since there are two imaging modes for MR imaging, T_1-weighted and T_2-weighted modes, contrast enhancers for both types need to be improved.

(a) T_1 contrast agents

There are mainly two ways to improve the T_1 efficiency: increase the intrinsic relaxivity and increase the number of probe sites.[99] Polymers, liposomes, virus capsids, perfluorocarbons and zeolites[98,100] have been employed to accumulate Gd complexes, resulting in higher efficiency. More recently, inorganic nanoparticles showed great potential as contrast agents.[101] Since conventional MRI contrast agents, $[Gd(DTPA)]^{2-}$ complex and its analogs do not enter cells with good efficiency, one may exploit MSNs as a carrier for Gd because of its efficient cell internalization capability and large surface area, which can accumulate huge number of Gd; thus, multifunctional

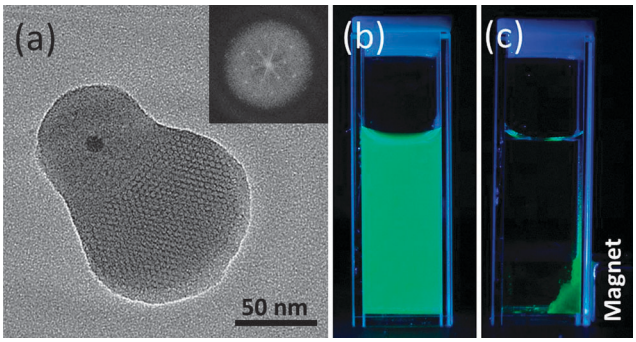

Fig. 5 (a) HR-TEM image of Mag-Dye@MSN. The inset is the Fourier transform pattern of porous structure. Photographs of aqueous suspension of Mag-Dye@MSN (b) under UV light irradiation, (c) after magnetic capture and under UV light irradiation. (Reproduced with permission from ref. 111. Copyright 2006, American Chemical Society).

mesoporous nanoparticles with MR and optical probes and porous property were synthesized.

The paramagnetic Gd(ph-NCS-DTPA) was employed as a T_1 contrast probe and was attached to MSNs internally to form Gd-Dye@MSN spheres[102] (*ca.* 120 nm spheres) and Gd-Dye@MSN-R (rods of 107 × 300–500 nm)[103] depending on the amount of ph-NCS-DTPA used in the co-condensation. Since there are 26637 Gd /rod in Gd-Dye@MSN-R, the effective r_1 is 26637 × 22 mM^{-1} s^{-1} on a per millimolar particle basis which is a significant improvement. Both functionalized mesoporous silicas were internalized efficiently to various cells in a concentration- and time-dependent way as for FITC-MSN. Phantom images of those MSNs demonstrated the feasibility of their use as cell-labelling agents. The labelling potential was further demonstrated *in vivo* with hMSC on nude mouse at 1.5 T.[102] With water freely flowing through the nanochannels, large number of Gd complexes inside the MSN, and saving the outer surface for targeting, MSNs should be an excellent platform for MRI cell-labelling. Taylor *et al.*[104] grafted poorly stable Si-DTTA-Gd onto MSNs in post-synthesis and were able to obtain high Gd-DTTA loading. Since DTTA is a heptadentate ligand, there are two water molecules binding to gadolinium; this increases the relaxivity, but decreases the stability of the complex. In addition, this two vacancies can be easily taken up by endogenous ligands such as phosphate and carbonate, and render lower r_1 values *in vivo*.[99] Recently, derivatives of the thermodynamic stable Gd-DOTA complex were anchored to the external surface of MSNs and manifested the interaction between the complex and silanol, depending on the structure.[105] It is interesting to note that SBA-15 and MCM-41 display quite different behaviour in the post-synthesis modification with Gd-DOTA; in the former, Gd-DOTA was anchored to the inner channel while on the outer surface for the latter, resulting in 4-fold lower r_1 for SBA-15 than that of MCM-41.[106]

Another approach to improve the T_1 relaxivity is to have very rigid backbones, reducing the rotational movement of metal. Thus Gd@MS was synthesized under acidic conditions where Gd was incorporated into the silica skeleton. Gd@MS displays a high and relatively field insensitive r_1.[107] Li *et al.*[108] reported that the adsorbed water molecules on the surface of Gd_2O_3@MCM-41 decrease with the increase in Gd doping by molecular dynamic simulation, and confirmed by experiments. However, the correlation between this trend and T_1 relaxivity was not examined. There are few molecular examples of restricted internal motion improvement on r_1.[99,109]

(b) T_2 contrast agents

Iron oxide is widely known for its role in T_2 contrast enhancement. Numerous preparations of iron oxide have been reported and applications demonstrated, yet, there are still advantages for magnetic mesoporous silica, especially in multifunctional targeted imaging and therapy.[110]

Superparamagnetic SPIO@SiO_2 was fused with FITC-MSN to form a first mesoporous silica based T_2 agent, Mag-Dye@MSN with fluorescence and MR imaging capability (Fig. 5).[111] This is different from most of the later reported ones, in that the pores are well ordered and the particle has a non-spherical tumbler shape. Mag-Dye@MSN exhibits high r_2, 153 mM^{-1} s^{-1}, in spite of its relatively low Fe content, about 1 wt%. Since these particles disperse very well in aqueous solution, both *in vitro* cell imaging and *in vivo* animal examinations were carried out with MR at 7 T field strength. It is interesting that a larger decrease in MRI signal in Mag-Dye@MSN treated hMSC cells was observed than that in SPIO@SiO_2-FITC[112], and Mag-Dye@MSN displayed a higher hMSC labelling efficiency than SPIO@SiO_2-FITC.[86]

Deng *et al.*[113] synthesized high-magnetization mesoporous silica spheres with perpendicular channels and demonstrated the removal of microcystins with these nanoparticles. Kim *et al.*[114] synthesized magnetic cores embedded in fluorescence labelled silica spheres with wormhole-like mesopores, and showed the accumulation of the nanoparticles in tumor bearing sites through an enhanced permeability and retention (EPR) effect in passive targeting. Liong *et al.*[89] managed to enclose multiple magnetites in the core, forming a multifunctional mesoporous silica (magnetic and fluorescence function), and demonstrated its targeted drug carrier function by carrying anticancer drugs to α-folate receptor over-expressed cells. Lee *et al.*[115] also demonstrated multimodal imaging and drug delivery with multiple magnetites decorated dye-MSN spheres.

Drug delivery

Mesoporous silica has a large surface area and pore volume and it can be easily functionalized. Naturally, it is most suitable for carrying drugs and biomolecules. A study on mesoporous silica as a drug carrier was first reported in 2001, using ibuprofen as a model drug, studied in simulated body fluid.[116] Since then, many studies on *ex vivo* drug delivery were reported and the parameters controlling the release profile were examined.[117] It was not until 2003 that drug delivery to cells using MSNs as a vehicle was reported.[69] The newer generation of MSN delivery systems focused on stimuli-responsive controlled release of drug or gated drug release, using removable nanoparticles to cap the pores and the caps be removed *via* redox reaction,[118] pH change,[119] or photo release.[120] Blocking the pores with photo-isomerizable compounds were also reported.[121,122] Recently, using the melting or enzyme digestion of DNA, researchers have been able to build stimulatable caps for pores to deliver drugs.[123–125]

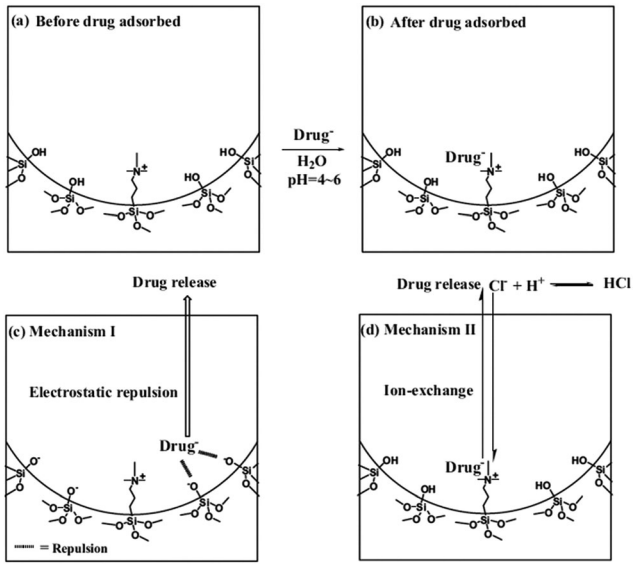

Fig. 6 Illustration of the sustained-release mechanism of an anionic drug adsorbed in MSN-TA sample. (a) Before drug adsorbed, (b) after drug adsorbed, (c) drug released by electrostatic repulsion under neutral pH, and (d) drug released by increasing the ionic strength. (Reproduced with permission from ref. 138. Copyright 2008, Wiley Publishing Company.)

Since MSNs can simultaneously carry many drugs with different physicochemical properties at high loading, the delivery of a cocktail of drugs will be its special advantage. Recently, Brinker and co-workers showed with combinations of therapeutic agents of drugs (doxorubicin and cisplatin), small interfering RNA and toxins, MSNs with a designed bilayer surface lipid coverage, enables a single protocell to kill a drug-resistant human hepatocellular carcinoma cell.[92] The field of drug delivery by MSNs has become very active and large. For recent progress, one can consult recent reviews.[120,126–129]

A different approach for controlled drug release involves generating a destructive species *in situ*. We used an external optical stimuli to generate singlet oxygen to annihilate cells, *i.e.* photodynamic therapy (PDT), which is a less invasive technique, and the resulting photodynamic effect can be limited to the area of interest, leaving the surrounding healthy tissues and cells undamaged.[130,131] Photosensitizer, protoporphyrin IX (PpIX) or Pd-porphyrin, was conjugated to MSNs through covalent bonding to yield sensitizer modified MSNs (PpIX-MSNs or PdPor-MSN). *In vitro* tests performed with HeLa cells revealed high cellular uptake efficiency and the phototoxicity was found to be both irradiation time- and dosage-dependent. PpIX-MSNs might be regarded as a controlled delivery system while cytotoxicity would occur only in the area where suitable light is irradiated. Light acts like a trigger to induce toxicity and this, in turn, causes subsequent cell damage or even death. Later, mannose-targeted MSN with covalent bonded porphyrin showed great PDT efficiency.[132] However, there is an optimal amount of mannose for the PDT efficiency, and a high density of mannose will lower the phototoxicity of the nanoparticles.[133]

More recently, a tri-functional MSN with imaging, targeting and therapy was developed.[134] A near-infrared fluorescent dye ATTO647N was incorporated to track the nanoparticles, cRGDyK peptide was attached to the outer surfaces of MSNs for targeting $\alpha_v\beta_3$ integrins of cancer cells, and palladium-porphyrin photosensitizer was incorporated to the channels for PDT. When U87-MG (human glioblastoma cells, $\alpha_v\beta_3^+$) and MCF-7 (human breast cancer cells, $\alpha_v\beta_3^-$ as a control) were treated with this assembly, A647@MSN-RGD-PdTPP, separately, only ~10% U87-MG cells survived irradiation while there was only ~20% loss for MCF-7. Thus, tri-functionalized MSNs can serve as a theranostic PDT platform.

pH-Responsive drug release is another active area. In order to deliver covalently bonded drugs, some environment sensitive release mechanism is often built into the drug–MSN assembly. An approach to generate active drug intracellularly is to use a pH-responsive hydrazone bond to attach drugs which can be cleaved in acidic endosome and the drugs released.[135] The anticancer drug doxorubicin was attached to MSN and TA-MSN (a more positively charged MSN to enhance the cell uptake) through hydrazone bonds. The release of doxorubicin was time- and pH dependent, with almost no release at pH 7.4. The effectiveness of these systems was tested against human hepatoma Hep-G2 cells, and the cell viability was reduced to 30% with positively charged TA-MSN-Hydrazone-Dox. This manifests the importance of cell uptake efficiency. Another pH responsive mechanism is the use of metal carboxylate complexes. Gu *et al.* designed a pH-responsive cisplatin release based on carboxylic acid functionalized MSNs.[136] Cysteine residue covalently attached to thiol-functional group could be released after glutathione reduction.[137] Particle-bound drugs attached by an amide linkage may be cleaved by protease in acidic compartment.[137]

We have also demonstrated positive-charge functionalized MSNs, MSN-TA, for oral drug delivery (Fig. 6).[138] The anionic prodrug sulfasalazine was electrostatically loaded into MSN-TA and remained inside MSN-TA under an acidic stomach environment. At pH 7.4, a partial negative surface charge on MSN-TA due to the deprotonation of silanol groups generated strong repulsion, so that the drug could be released in the intestines. In the simulated intestinal fluid (pH 7.4), the release rate was regulated by the surface charge, *i.e.* the amount of TA (trimethylammonium) groups.

In vivo MSN drug delivery was demonstrated with phosphonated FMSN with and without folic targeting ligand carrying camptothecin, an anticancer drug. Both formulations showed MSNs accumulated in the tumor site of the mice with MCF-7 xenografts and effectively reduced the tumor. However, little difference between folic and non-folic functionalized MSNs in the *in vivo* efficacy was observed.[139]

An important problem encountered in chemotherapy is the multiple drug resistance (MDR), including so-called "pump" and "nonpump" resistance, in cancer cells. However, further functionality can be built on MSNs for overcoming MDR.[140,141] Co-delivery strategies that utilize Pgp siRNA or Bcl-2 siRNA to suppress, respectively, the drug efflux (pump resistance) or activation of cellular antiapoptotic defense (nonpump resistance), together with an anticancer drug, have been developed for MDR cancer cells.[140,141] The use of pH-responsive MSN carrying doxorubicine to antagonize cancer MDR with pronounced *in vivo* therapeutic effect was also successfully demonstrated for the first time.[142]

Degradation, toxicity, biodistribution and clearance

Many biomedical applications of MSNs such as cell labelling, drug delivery, diagnostic imaging, bone tissue regeneration, *etc*. have been demonstrated. For further *in vivo* biological considerations, biocompatibility has to be exhaustively examined; this includes biodegradation, toxicity, biodistribution and clearance, to name a few.

It is crucial to know if the nanoparticle is biodegradable because how it is applied depends heavily on this property. He *et al*.[143] reported that surfactant-extracted mesoporous silica degrades in a three-stage fashion in simulated body fluid (SBF), that is, a very fast degradation within two hours, followed by a silicon concentration decrease stage (due to silicate deposition, forming a passivating layer) and last, a very slow degradation. After 15 days, this degradation is almost finished. The degradation depends on the initial concentration and specific surface area. On the contrary, calcined mesoporous silica does not degrade as much, only to about 32%, however, a fast initial degradation was also observed. Similar fast degradation to monomeric or dimeric silicic acid species was also reported for calcined porous silica films.[144] On the other hand, non-porous sol–gel silica has relatively low degradation and showed no well-defined stages.[143] Indeed, the large amount of urine excretion within one day post injection of MSN *vide infra*[139,145] is in accord with this fast first stage degradation.

Stirring functionalized (phenyl, aminopropyl and chloropropyl) mesoporous silica nanoparticles in the size range of 50–70 nm in SBF at 37 °C for one month showed partial degradation between first 2 and 24 h. After 1 month, pore blocking occurred along with the deposition of hydroxyapatite (HAp) needles on the surface. However, PEG-silane (M.W. 550) coated MSNs had better stability within the first day of soaking, but after 1 month, pore blocking and reduction of structural features still occurred.[146] An opposite stability trend between calcined SBA-15 and aminopropyl, methyl and octyl functionalized SBA-15 was reported recently.[147] Since those SBA-15 materials were prepared under acidic conditions, while MCM-41 type MSNs were synthesized under basic conditions, the preparation method may interfere with a direct comparison. Lin *et al*.[148] compared the amount of degraded free Si between PEGylated MSN and MSN after 10 days of aging in de-ionized water and PBS at room temperature or at 37 °C. In each case, PEGylation gave less degradation and better biocompatibility. Therefore, PEGylation retarded the degradation of porous silica, and hydrothermal treatment can further improve stability.

(a) Cell level toxicity

Cytotoxicity depends on cell type, particle size and shape, surface chemistry and aggregation state.[149] For nanoparticles, it is important to choose a fully satisfactory test for biocompatibility, for example a MTT test is not suitable for nanosilicon due to the oxidation/reduction, but is valid for silica from the redox aspect.[150] However, Fisichella *et al*.[151] reported that in some cells, MSNs promote the exocytosis of formazan crystals and MTT assay overestimates the cytotoxicity of MSNs. Most of the cell toxicity reported was studied with MTT or LDH assays for a short period; a few examined biochemical responses such as cellular respiration,[152] immunogenicity,[153] blood compatibility,[87,154,155] cell adhesion and migration,[80] and cell function of secretion.[156] There are few studies related to the size effect on cytotoxicity in the drug delivery relevant range, *i.e*. 200 nm or less.[155] Most studies compared micro- *vs*. nano-sized porous silica.[65,153] In addition, the fabrication method affects the nature of the nanoparticles, making a direct comparison problematic. More systematic study on cytotoxicity is highly desirable.

It is reported that porous silica biodegrades to monomeric and oligomeric silicic acids and those products are not cytotoxic.[65] Thus, the internalization of FITC-MSNs (110 nm) did not affect the cell viability, proliferation, immunophenotype and differentiation potential of mesenchymal stem cells (hMSC) and 3T3-L1 cells.[48] On the other hand, a transient upregulation of actin cytoskeletal organization was detected.[157] Initial MTT assay on a series of MSNs from 300 nm down to 30 nm did not show acute toxicity to HeLa cells.[49] However, hemolysis studies showed that smaller MSNs are more toxic due to better uptake to cells and more silanol groups available for cell contacting.[155] The surface silanol groups have been proposed as the cause for hemolysis.[87] Thus, MSNs shows lower hemolysis activity due to its hollow surface and less silanol interacting with cell membrane. Similarly surface functionalized MSNs, especially with PEG, are less toxic to cells.[155,158] It has also been shown the interaction between MSNs and red blood cells is size-dependent, with the larger SBA-15 type MSNs showing stronger membrane deformation and eventual hemolysis.[159]

Since cell stress is usually related to the generation of reactive oxygen species (ROS), particle-induced oxidative stress is proposed as a paradigm for toxicity of silica.[160] The cellular respiration of mouse tissue was not affected by calcined MCM-41 and SBA-15;[161] but for the solvent extracted mesoporous silica, cellular response depends on pore size. Its smaller pores may limit entry of essential biomolecules, and thus MCM-41 has only a small effect on cellular respiration. However, SBA-15 inhibited cellular respiration at 25–500 μg mL^{-1}.[152] Unlike silica nanoparticles,[162] both types of mesoporous nanoparticles had no effect on the cellular glutathione indicating that ROS was not involved in the O_2 consumption. It is also reported that there is no direct correlation between ROS generation and the cytotoxicity.[163]

A good example of cytotoxicity depending on cell type is manifested in that MSNs promote only the growth of A375 (human malignant melanoma cells) not HEK293T, HMEC or MDA-MB-231, due to a decrease in ROS. The tumor growth promotion was also observed *in vivo*.[164] Thus, one has to be cautious on drawing conclusions on cytotoxicity since the particle preparation, size, state of aggregation and surface chemistry, all will affect the interactions between particles and cells, on top of different cell types. There is a need to have standardized methods on assessing cytotoxicity of porous silica materials.[163]

(b) Animal level

The first *in vivo* animal study of mesoporous silica nanoparticles was carried out with magnetic mesoporous silica nanoparticles administered to mice and no adverse effect was observed.[165] After i.v. injection of Mag-Dye@MSN in a dosage of

2 mg Fe kg^{-1} (body weight), mice did not exhibit any abnormal clinical signs, and their body weights also appeared normal comparing with the control during a four-week study period. Hudson *et al.*[9] reported that porous silica were lethal to mice when intra-peritoneal and intra-venous injected in mice, but no toxicity was observed with subcutaneous injection in mice. This may be due to the very high dosage (1.2 g kg^{-1}), large particle size, and particle preparation in the work; indeed blood clogging was suspected for the death. In subcutaneous injected mesoporous silicates, the residual material decreased progressively over 3 months with good biocompatibility.[9]

Extensive long-term studies of 14 days and 2 months were carried out on mice by Lu *et al.*[139] They examined blood samples and tissues and performed physical observations of phosphonate-FMSN (100–130 nm) treated mice. Fourteen days after nanoparticle-injection, the mice appeared healthy, and neither histological lesion in the tissues nor pathological abnormalities in major organs were detected. Three mice showed mild inflammation at the 14th day and one showed slightly high eosinophil count and impaired liver function. Results of two months long-term studies showed that treated mice had no abnormality in hematology or histopathology results or lesions related to the nanoparticles treatments, except two mice had mildly elevated liver function indexes and one had mild gastritis. Tamanoi and co-workers[139] also did not find an apparent effect in mice over a long observation period of 68 days at a higher total dose level of 1 mg/mouse/day. Dosage of 50 mg kg^{-1} has been suggested for pharmacological applications.[139] This is an encouraging result.

In addition, toxicity studies on mesoporous hollow silica (110 nm, MHSN) with single i.v. injection to mice showed LD_{50} > 1000 mg kg^{-1}.[166] Furthermore, continuous i.v. injection for 14 d at 20, 40 and 80 mg kg^{-1} resulted in no death, and no abnormalities were detected in the liver, spleen and kidneys for 20 mg kg^{-1} dose.[166] The excretion time for MHSN was estimated to be more than 4 weeks. Micron sized tetraethylene glycol functionalized acid-prepared mesoporous silica spheres were also exploited as a drug carrier through intranasal and intrapleural routes. *In vivo* test results were encouraging in that no immunogenic and toxicity were observed.[167]

(c) Biodistribution and clearance

It is known that the particle size, charge and surface chemistry will affect the pharmacokinetics and biodistribution.[168] Early on; we used MRI to investigate the biodistribution of Mag-Dye@MSN in mice.[165] The time-dependent darkening of the MR images at the liver, spleen and kidneys after administration of Mag-Dye@MSN showed the recovery time of signal-to-noise ratio (SNR) in the kidneys was notably shorter than that in liver/spleen suggesting that most Mag-Dye@MSN were trapped by the RES organs. Long-term MRI tracking study indicated that the negatively charged Mag-Dye@MSN could be trapped in the liver as long as three months. However, recently Lu *et al.*[139] in a study of biodistribution of negatively charged MSNs found that most of MSNs excreted through urine (major) and feces (minor) in 4 days after injection. This indicates quick dissolution of MSNs in the body. The Mag-Dye@MSN contains a non-porous silica part (see Fig. 5a).[165] A reasonable explanation would be that mesoporous silica can be digested much quicker than solid nonporous silica particles.[143]

Real-time monitoring of *in vivo* biodistribution was demonstrated with MSN-TA-ICG, where indocyanine green, a negative NIR dye, was electrostatically incorporated to MSN-TA (50–100 nm in size), resulting in MSN-TA-ICG of ξ-potential −17.6 mV.[72] *In vivo* imaging and ICP-AES quantitative elemental analysis on organs manifested the nanoparticles mainly in the liver, and to a lesser extent in the kidneys, lungs, spleen and heart. On the other hand, MSN-NH_2-ICG (50–100 nm in size), which had covalently bonded ICG and ξ-potential of +34.4 mV at pH 7.4, revealed a dramatically different behaviour.[169] Within 10 min of tail vein injection, almost all nanoparticles appeared in the liver, and 60 min later a significant amount moved to the duodenum *via* the biliary duct (Fig. 7). Four hours after administration of nanoparticles, *in vivo* images displayed that most MSNs were in the jejunum and duodenum, with only a modest amount left in the liver. *Ex vivo* fluorescence imaging of harvested organs and ICP-MS quantification of silica confirmed these observations. Silica content in feces was >60% than that of the control in each of 3 days post nanoparticles injection, and peaked on day 2 post-treatment. No silica was detected in the urine. In addition, data on 3 days after injection indicated that MSN excretion was still ongoing, but at a far reduced rate. Hence, the *in vivo* clearance of the nanoparticles is surface charge dependent, the clearance of positively charged particles started within 30 min post administration, while lower surface charged MSNs remained in the body for days longer.

Faure *et al.*[170] explored the ξ-potential effect on the biodistribution of small PEGylated Gd_2O_3 (hydrodynamic diameter <20 nm). They found that positive-charged nanoparticles (amine terminated PEG) accumulated in the liver, spleen and intestine, which indicated excretion by feces while $-CO_2H$ and $-OCH_3$ terminated PEG nanoparticles did not accumulate in those organs.

Lu *et al.*[139] examined the biodistribution and excretion of phosphonate-MSN, FMSN. Urine and feces were collected and Si content was analyzed with ICP-OES. Almost all of silicon injected was excreted out through urine (major) and feces in 4 d (94.4%). PEG coated nanoparticles can increase the *in vivo* circulation time, with a half-life up to 3 h (PEG-phospholipid micelles)[171] as compared to NP without a PEG coating, with a half-life of about 15 min.[172] The density and molecular weight of surface PEG will affect the extent of human serum protein binding.[173] Moreover, the effective chain length varies with cell type due to the cell-type dependent nonspecific binding (studied in the case of Q dots).[174] He *et al.*[145] monitored the biodistribution and urinary excretion of a series of 80–360 nm MSNs and corresponding PEG-MSN for 1 month. The liver and spleen are the main organs where both type of nanoparticles lodged, whereas less particles were found in the lung, and even less in the kidneys and heart. However, the amount of PEG-MSN in the liver, spleen and lung are lower than that in the MSN case. This is in accordance with the known PEG effect which would prevent the phagocytes to recognize and remove the nanoparticles from the circulation. Here, we see that PEG exerts more effect on the larger particles than the small ones, especially in the

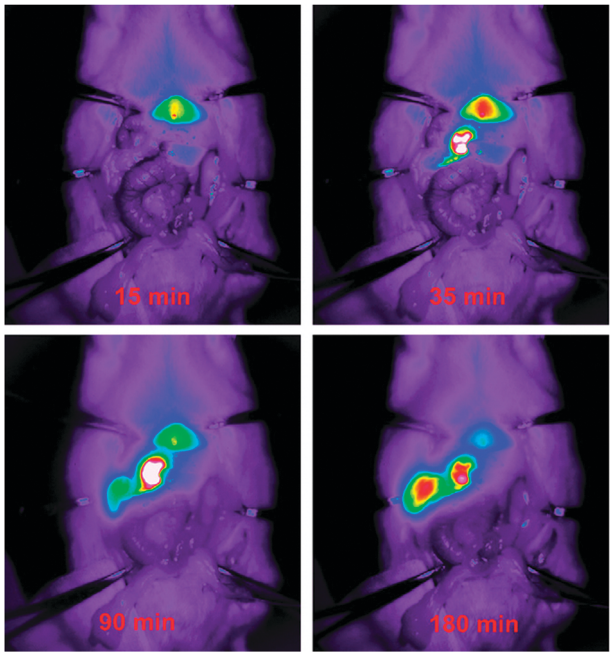

Fig. 7 Hepatobiliary dynamic transport of MSN-NH_2-ICG from circulation into the GI tract in an anesthetized rat following i.v. injection. Within 10 min of injection nearly all of the MSN-NH_2-ICG has been sequestered by the liver. After 30 min a substantial percentage of MSN-NH_2-ICG has already begun to migrate into the GI tract. (Reproduced with permission from ref. 169. Copyright 2010, Elsevier Inc.)

lung. Urinary excretion of all sized MSN and PEG-MSN were observed, similar to Lu's investigation.[139] It is worth noting that the urine excreted in the first 30 min was very high for larger MSNs (45% for 360 nm MSNs), in tune with the fast degradation of larger MSNs in simulated body fluid, *vide supra*. It is amazing the nanoparticles are excreted through the urine since it is known that only particles less than 5.5 nm can be excreted through the kidneys.[175] On the other hand, silica spheres were also reported to be excreted through the kidneys.[176,177] Hence, the fate of mesoporous silica *in vivo* is both biodegradation and excretion through urine or bile ducts.

Conclusion and perspectives

Mesoporous silica nanoparticles can be fabricated with various sizes and shapes. Because of their versatile pore structure and functionality, design strategies for targeting specific tissue/cell are rich and MSNs have a high potential in nanomedicine. Although there have been tremendous efforts in the synthesis of uniform-sized MSNs, still more efforts are needed in the synthesis of truly dispersible uniform-sized nanoparticles with tuneable pore sizes from a few nm to large pores, to accommodate various applications such as drug delivery for small molecules through to DNA plasmids. Thorough understanding of the physical and chemical properties of the nanoparticles (including the functionalized MSNs), especially stability towards degradation/no degradation are still lacking. In addition, care should be taken to isolate the nanoparticles without changing the colloidal stability and state of aggregation, separation process such as dialysis, which does not alter the aggregation state, should be used for materials preparation.

Enhancing drug deliveries at specific cells and sub-cellular organelles by taking advantage of the endocytotic pathways and intracellular trafficking mechanisms are still in early stages of development.[12] Better understanding of the structure-organelle escaping relationship is needed for designing efficient drug delivery/transfection. For this purpose, more new methods of MSN functionalization for building multi-modality are needed. Mechanisms such as capping for intelligent delivery will be helpful in providing such methods. Imaging cell activity with various sensors, pH and ion sensing for example, may be built on MSNs to understand intracellular activity. These developments in multi-functionality will bring MSNs into the mainstream multi-disciplinary research of nanomedicine. In the cell level studies, exocytosis of nanoparticles has been rarely studied. However, this is very desired for drug delivery to overcome multidrug resistance and for slow drug release, the drug reservoir (the nanoparticles) should remain in the cells long enough for the effect.

Presently, some conflicting data related to toxicity have been reported, which may be caused by different preparations, size, dosage, *etc*. This calls for a standard protocol for particle-treatments and toxicity investigation. In addition, interactions between the nanoparticles and cells, although very complicated, merit more efforts to understand them.

As the biological applications of MSNs are burgeoning, more *in vivo* studies will be invoked. An urgent issue is the biodegradability of MSNs and its derivatives *in vivo*. Animal-level demonstration of proposed *ex vivo* targeted delivery of drugs/biomolecules is required before MSNs can be considered further. Nevertheless, results on recent *in vivo* biodistribution studies are very encouraging and warrant further development of MSNs.

Acknowledgements

The authors thank the National Project of Nanotechnology under National Science Council of Taiwan for the support of their researches. We thank Dr Leu-Wei Lo and Mr Yu-Shen Lin for valuable suggestions.

References

1 B. Y. S. Kim, J. T. Rutka and W. C. W. Chan, *N. Engl. J. Med.*, 2010, **363**, 2434–2443.
2 V. Biju, T. Itoh and M. Ishikawa, *Chem. Soc. Rev.*, 2010, **39**, 3031–3056.
3 J. Gao, H. Gu and B. Xu, *Acc. Chem. Res.*, 2009, **42**, 1097–1107.
4 A. H. Lu, E. L. Salabas and F. Schüth, *Angew. Chem., Int. Ed.*, 2007, **46**, 1222–1244.
5 C. Burda, X. B. Chen, R. Narayanan and M. A. El-Sayed, *Chem. Rev.*, 2005, **105**, 1025–1102.
6 I. I. Slowing, J. L. Vivero-Escoto, B. G. Trewyn and V. S. Y. Lin, *J. Mater. Chem.*, 2010, **20**, 7924–7937.
7 B. G. Trewyn, S. Giri, I. I. Slowing and V. S. Y. Lin, *Chem. Commun.*, 2007, 3236–3245.
8 Q. He and J. Shi, *J. Mater. Chem.*, 2011, **21**, 5845–5855.
9 S. P. Hudson, R. F. Padera, R. Langer and D. S. Kohane, *Biomaterials*, 2008, **29**, 4045–4055.
10 D. Bruhwiler, *Nanoscale*, 2010, **2**, 887–892.
11 T. H. Chung, S. H. Wu, M. Yao, C. W. Lu, Y. S. Lin, Y. Hung, C. Y. Mou, Y. C. Chen and D. M. Huang, *Biomaterials*, 2007, **28**, 2959–2966.

12 L. Y. T. Chou, K. Ming and W. C. W. Chan, *Chem. Soc. Rev.*, 2011, **40**, 233–245.
13 M. Manzano and M. Vallet-Regi, *J. Mater. Chem.*, 2010, **20**, 5593–5604.
14 M.-H. Kim, H.-K. Na, Y.-K. Kim, S.-R. Ryoo, H. S. Cho, K. E. Lee, H. Jeon, R. Ryoo and D.-H. Min, *ACS Nano*, 2011, **5**, 3568.
15 C. H. Lee, T. S. Lin and C. Y. Mou, *Nano Today*, 2009, **4**, 165–179.
16 M. Grun, I. Lauer and K. K. Unger, *Adv. Mater.*, 1997, **9**, 254–257.
17 R. I. Nooney, D. Thirunavukkarasu, Y. M. Chen, R. Josephs and A. E. Ostafin, *Chem. Mater.*, 2002, **14**, 4721–4728.
18 Q. Cai, Z. S. Luo, W. Q. Pang, Y. W. Fan, X. H. Chen and F. Z. Cui, *Chem. Mater.*, 2001, **13**, 258–263.
19 K. Suzuki, K. Ikari and H. Imai, *J. Am. Chem. Soc.*, 2004, **126**, 462–463.
20 Y. Han and J. Y. Ying, *Angew. Chem., Int. Ed.*, 2005, **44**, 288–292.
21 C. Urata, Y. Aoyama, A. Tonegawa, Y. Yamauchi and K. Kuroda, *Chem. Commun.*, 2009, 5094–5096.
22 Q. He, X. Cui, F. Cui, L. Guo and J. Shi, *Microporous Mesoporous Mater.*, 2009, **117**, 609–616.
23 H. I. Lee, J. H. Kim, G. D. Stucky, Y. Shi, C. Pak and J. M. Kim, *J. Mater. Chem.*, 2010, **20**, 8483–8487.
24 A. Berggren and A. E. C. Palmqvist, *J. Phys. Chem. C*, 2008, **112**, 732–737.
25 Q. He, J. Shi, J. Zhao, Y. Chen and F. Chen, *J. Mater. Chem.*, 2009, **19**, 6498–6503.
26 C. E. Fowler, D. Khushalani, B. Lebeau and S. Mann, *Adv. Mater.*, 2001, **13**, 649–652.
27 K. Moller, J. Kobler and T. Bein, *Adv. Funct. Mater.*, 2007, **17**, 605–612.
28 Y. Yamada and K. Yano, *Microporous Mesoporous Mater.*, 2006, **93**, 190–198.
29 T. Suteewong, H. Sai, R. Cohen, S. Wang, M. Bradbury, B. Baird, S. M. Gruner and U. Wiesner, *J. Am. Chem. Soc.*, 2011, **133**, 172–175.
30 Y. Lu, H. Fan, A. Stump, T. L. Ward, T. Rieker and C. J. Brinker, *Nature*, 1999, **398**, 223–226.
31 S. R. Zhai and C. S. Ha, *Microporous Mesoporous Mater.*, 2007, **102**, 212–222.
32 K. Ikari, K. Suzuki and H. Imai, *Langmuir*, 2006, **22**, 802–806.
33 T. W. Kim, P. W. Chung and V. S. Y. Lin, *Chem. Mater.*, 2010, **22**, 5093–5104.
34 L. Zhang, S. Z. Qiao, Y. G. Jin, Z. G. Chen, H. C. Gu and G. Q. Lu, *Adv. Mater.*, 2008, **20**, 805–809.
35 X. J. Wu and D. Xu, *Adv. Mater.*, 2010, **22**, 1516–1520.
36 D. Niu, Z. Ma, Y. Li and J. Shi, *J. Am. Chem. Soc.*, 2010, **132**, 15144–15147.
37 Y. Q. Yeh, B. C. Chen, H. P. Lin and C. Y. Tang, *Langmuir*, 2006, **22**, 6–9.
38 Z. Feng, Y. Li, D. Niu, L. Li, W. Zhao, H. Chen, L. Li, J. Gao, M. Ruan and J. Shi, *Chem. Commun.*, 2008, 2629–2631.
39 J. G. Wang, F. Li, H. J. Zhou, P. C. Sun, D. T. Ding and T. H. Chen, *Chem. Mater.*, 2009, **21**, 612–620.
40 X. Liu, P. Wang, L. Zhang, J. Yang, C. Li and Q. Yang, *Chem.–Eur. J.*, 2010, **16**, 12727–12735.
41 J. Liu, S. B. Hartono, Y. G. Jin, Z. Li, G. Q. Lu and S. Z. Qiao, *J. Mater. Chem.*, 2010, **20**, 4595–4601.
42 C. C. Huang, W. Huang and C. S. Yeh, *Biomaterials*, 2011, **32**, 556–564.
43 Y. Chen, H. Chen, L. Guo, Q. He, F. Chen, J. Zhou, J. Feng and J. Shi, *ACS Nano*, 2010, **4**, 529–539.
44 Y. S. Lin, S. H. Wu, C. T. Tseng, Y. Hung, C. Chang and C. Y. Mou, *Chem. Commun.*, 2009, 3542–3544.
45 Z. Teng, Y. Han, J. Li, F. Yan and W. Yang, *Microporous Mesoporous Mater.*, 2010, **127**, 67–72.
46 J. Zhu, J. Tang, L. Zhao, X. Zhou, Y. Wang and C. Yu, *Small*, 2010, **6**, 276–282.
47 J. Liu, S. Bai, H. Zhong, C. Li and Q. Yang, *J. Phys. Chem. C*, 2010, **114**, 953–961.
48 Y. S. Lin, C. P. Tsai, H. Y. Huang, C. T. Kuo, Y. Hung, D. M. Huang, Y. C. Chen and C. Y. Mou, *Chem. Mater.*, 2005, **17**, 4570–4573.
49 F. Lu, S. H. Wu, Y. Hung and C. Y. Mou, *Small*, 2009, **5**, 1408–1413.
50 X. G. Peng, J. Wickham and A. P. Alivisatos, *J. Am. Chem. Soc.*, 1998, **120**, 5343–5344.
51 Y. S. Lin, C. Y. D. Lu, Y. Hung and C. Y. Mou, *ChemPhysChem*, 2009, **10**, 2628–2632.
52 S. Huh, J. W. Wiench, B. G. Trewyn, S. Song, M. Pruski and V. S. Y. Lin, *Chem. Commun.*, 2003, 2364–2365.
53 S. Huh, J. W. Wiench, J. C. Yoo, M. Pruski and V. S. Y. Lin, *Chem. Mater.*, 2003, **15**, 4247–4256.
54 N. Lang and A. Tuel, *Chem. Mater.*, 2004, **16**, 1961–1966.
55 M. C. Burleigh, M. A. Markowitz, M. S. Spector and B. P. Gaber, *J. Phys. Chem. B*, 2001, **105**, 9935–9942.
56 M. H. Lim and A. Stein, *Chem. Mater.*, 1999, **11**, 3285–3295.
57 C. Zapilko, M. Widenmeyer, I. Nagl, F. Estler, R. Anwander, G. Raudaschl-Sieber, O. Groeger and G. Engelhardt, *J. Am. Chem. Soc.*, 2006, **128**, 16266–16276.
58 H. Ritter and D. Brühwiler, *J. Phys. Chem. C*, 2009, **113**, 10667–10674.
59 W. H. Zhang, X. B. Lu, J. H. Xiu, Z. L. Hua, L. X. Zhang, M. Robertson, J. L. Shi, D. S. Yan and J. D. Holmes, *Adv. Funct. Mater.*, 2004, **14**, 544–552.
60 H. P. Lin, L. Y. Yang, C. Y. Mou, S. B. Liu and H. K. Lee, *New J. Chem.*, 2000, **24**, 253–255.
61 Y. H. Liu, H. P. Lin and C. Y. Mou, *Langmuir*, 2004, **20**, 3231–3239.
62 A. E. Nel, L. Madler, D. Velegol, T. Xia, E. M. V. Hoek, P. Somasundaran, F. Klaessig, V. Castranova and M. Thompson, *Nat. Mater.*, 2009, **8**, 543–557.
63 I. Slowing, B. G. Trewyn and V. S. Y. Lin, *J. Am. Chem. Soc.*, 2006, **128**, 14792–14793.
64 T. Xia, M. Kovochich, M. Liong, H. Meng, S. Kabehie, S. George, J. I. Zink and A. E. Nel, *ACS Nano*, 2009, **3**, 3273–3286.
65 Q. J. He, Z. W. Zhang, Y. Gao, J. L. Shi and Y. P. Li, *Small*, 2009, **5**, 2722–2729.
66 J. Lu, M. Liong, J. I. Zink and F. Tamanoi, *Small*, 2007, **3**, 1341–1346.
67 Y. Ma, L. Xing, H. Zheng and S. Che, *Langmuir*, 2011, **27**, 517–520.
68 C. P. Tsai, C. Y. Chen, Y. Hung, F. H. Chang and C. Y. Mou, *J. Mater. Chem.*, 2009, **19**, 5737–5743.
69 C. Y. Lai, B. G. Trewyn, D. M. Jeftinija, K. Jeftinija, S. Xu, S. Jeftinija and V. S. Y. Lin, *J. Am. Chem. Soc.*, 2003, **125**, 4451–4459.
70 J. M. Rosenholm, A. Duchanoy and M. Linden, *Chem. Mater.*, 2008, **20**, 1126–1133.
71 V. Cauda, A. Schlossbauer, J. Kecht, A. Zurner and T. Bein, *J. Am. Chem. Soc.*, 2009, **131**, 11361–11370.
72 C. H. Lee, S. H. Cheng, Y. J. Wang, Y. C. Chen, N. T. Chen, J. Souris, C. T. Chen, C. Y. Mou, C. S. Yang and L. W. Lo, *Adv. Funct. Mater.*, 2009, **19**, 215–222.
73 D. M. Huang, Y. Hung, B. S. Ko, S. C. Hsu, W. H. Chen, C. L. Chien, C. P. Tsai, C. T. Kuo, J. C. Kang, C. S. Yang, C. Y. Mou and Y. C. Chen, *FASEB J.*, 2005, **19**, 2014–2016.
74 T. Xia, M. Kovochich, M. Liong, J. I. Zink and A. E. Nel, *ACS Nano*, 2008, **2**, 85–96.
75 J. Rejman, V. Oberle, I. S. Zuhorn and D. Hoekstra, *Biochem. J.*, 2004, **377**, 159–169.
76 F. Osaki, T. Kanamori, S. Sando, T. Sera and Y. Aoyama, *J. Am. Chem. Soc.*, 2004, **126**, 6520–6521.
77 B. D. Chithrani and W. C. W. Chan, *Nano Lett.*, 2007, **7**, 1542–1550.
78 B. D. Chithrani, A. A. Ghazani and W. C. W. Chan, *Nano Lett.*, 2006, **6**, 662–668.
79 W. Jiang, B. Y. S. Kim, J. T. Rutka and W. C. W. Chan, *Nat. Nanotechnol.*, 2008, **3**, 145–150.
80 X. L. Huang, X. Teng, D. Chen, F. Q. Tang and J. Q. He, *Biomaterials*, 2010, **31**, 438–448.
81 Z. M. Tao, B. B. Toms, J. Goodisman and T. Asefa, *Chem. Res. Toxicol.*, 2009, **22**, 1869–1880.
82 S. D. Conner and S. L. Schmid, *Nature*, 2003, **422**, 37–44.
83 A. Verma, O. Uzun, Y. H. Hu, Y. Hu, H. S. Han, N. Watson, S. L. Chen, D. J. Irvine and F. Stellacci, *Nat. Mater.*, 2008, **7**, 588–595.
84 R. G. Flemming, C. J. Murphy, G. A. Abrams, S. L. Goodman and P. F. Nealey, *Biomaterials*, 1999, **20**, 573–588.

85 N. Krasteva, B. Seifert, W. Albrecht, T. Weigel, M. Schossig, G. Altankov and T. Groth, *Biomaterials*, 2004, **25**, 2467–2476.
86 H. M. Liu, S. H. Wu, C. W. Lu, M. Yao, J. K. Hsiao, Y. Hung, Y. S. Lin, C. Y. Mou, C. S. Yang, D. M. Huang and Y. C. Chen, *Small*, 2008, **4**, 619–626.
87 Slowing II, C. W. Wu, J. L. Vivero-Escoto and V. S. Y. Lin, *Small*, 2009, **5**, 57–62.
88 A. S. Zahr, C. A. Davis and M. V. Pishko, *Langmuir*, 2006, **22**, 8178–8185.
89 M. Liong, J. Lu, M. Kovochich, T. Xia, S. G. Ruehm, A. E. Nel, F. Tamanoi and J. I. Zink, *ACS Nano*, 2008, **2**, 889–896.
90 I. Y. Park, I. Y. Kim, M. K. Yoo, Y. J. Choi, M. H. Cho and C. S. Cho, *Int. J. Pharm.*, 2008, **359**, 280–287.
91 C. L. Zhu, X. Y. Song, W. H. Zhou, H. H. Yang, Y. H. Wen and X. R. Wang, *J. Mater. Chem.*, 2009, **19**, 7765–7770.
92 C. E. Ashley, E. C. Carnes, G. K. Phillips, D. Padilla, P. N. Durfee, P. A. Brown, T. N. Hanna, J. Liu, B. Phillips, M. B. Carter, N. J. Carroll, X. Jiang, D. R. Dunphy, C. L. Willman, D. N. Petsev, D. G. Evans, A. N. Parikh, B. Chackerian, W. Wharton, D. S. Peabody and C. J. Brinker, *Nat. Mater.*, 2011, **10**, 389–397.
93 J. P. Behr, *Chimia*, 1997, **51**, 34–36.
94 A. Dehshahri, R. K. Oskuee, W. T. Shier, A. Hatefi and M. Ramezani, *Biomaterials*, 2009, **30**, 4187–4194.
95 S. b. Febvay, D. M. Marini, A. M. Belcher and D. E. Clapham, *Nano Lett.*, 2010, **10**, 2211–2219.
96 A. M. Sauer, A. Schlossbauer, N. Ruthardt, V. Cauda, T. Bein and C. Brauchle, *Nano Lett.*, 2010, **10**, 3684–3691.
97 D. N. Nguyen, J. J. Green, J. M. Chan, R. Langer and D. G. Anderson, *Adv. Mater.*, 2009, **21**, 847–867.
98 E. Terreno, D. D. Castelli, A. Viale and S. Aime, *Chem. Rev.*, 2010, **110**, 3019–3042.
99 P. Caravan, *Chem. Soc. Rev.*, 2006, **35**, 512–523.
100 M. Tsotsalas, M. Busby, E. Gianolio, S. Aime and L. De Cola, *Chem. Mater.*, 2008, **20**, 5888–5893.
101 H. B. Na, I. C. Song and T. Hyeon, *Adv. Mater.*, 2009, **21**, 2133–2148.
102 J.-K. Hsiao, C.-P. Tsai, T.-H. Chung, Y. Hung, M. Yao, H.-M. Liu, C.-Y. Mou, C.-S. Yang, Y.-C. Chen and D.-M. Huang, *Small*, 2008, **4**, 1445–1452.
103 C. P. Tsai, Y. Hung, Y. H. Chou, D. M. Huang, J. K. Hsiao, C. Chang, Y. C. Chen and C. Y. Mou, *Small*, 2008, **4**, 186–191.
104 K. M. L. Taylor, J. S. Kim, W. J. Rieter, H. An, W. L. Lin and W. B. Lin, *J. Am. Chem. Soc.*, 2008, **130**, 2154–2155.
105 F. Carniato, L. Tei, M. Cossi, L. Marchese and M. Botta, *Chem.–Eur. J.*, 2010, **16**, 10727–10734.
106 F. Carniato, L. Tei, W. Dastru, L. Marchese and M. Botta, *Chem. Commun.*, 2009, 1246–1248.
107 Y. S. Lin, Y. Hung, J. K. Su, R. Lee, C. Chang, M. L. Lin and C. Y. Mou, *J. Phys. Chem. B*, 2004, **108**, 15608–15611.
108 S. A. Li, H. A. Liu, L. Li, N. Q. Luo, R. H. Cao, D. H. Chen and Y. Z. Shao, *Appl. Phys. Lett.*, 2011, 98.
109 F. Kielar, L. Tei, E. Terreno and M. Botta, *J. Am. Chem. Soc.*, 2010, **132**, 7836–7837.
110 J. Liu, S. Z. Qiao, Q. H. Hu and G. Q. Lu, *Small*, 2011, **7**, 418–418.
111 Y. S. Lin, S. H. Wu, Y. Hung, Y. H. Chou, C. Chang, M. L. Lin, C. P. Tsai and C. Y. Mou, *Chem. Mater.*, 2006, **18**, 5170–5172.
112 C. W. Lu, Y. Hung, J. K. Hsiao, M. Yao, T. H. Chung, Y. S. Lin, S. H. Wu, S. C. Hsu, H. M. Liu, C. Y. Mou, C. S. Yang, D. M. Huang and Y. C. Chen, *Nano Lett.*, 2007, **7**, 149–154.
113 Y. Deng, D. Qi, C. Deng, X. Zhang and D. Zhao, *J. Am. Chem. Soc.*, 2008, **130**, 28–29.
114 J. Kim, H. S. Kim, N. Lee, T. Kim, H. Kim, T. Yu, I. C. Song, W. K. Moon and T. Hyeon, *Angew. Chem., Int. Ed.*, 2008, **47**, 8438–8441.
115 J. E. Lee, N. Lee, H. Kim, J. Kim, S. H. Choi, J. H. Kim, T. Kim, I. C. Song, S. P. Park, W. K. Moon and T. Hyeon, *J. Am. Chem. Soc.*, 2010, **132**, 552–557.
116 M. Vallet-Regi, A. Ramila, R. P. del Real and J. Perez-Pariente, *Chem. Mater.*, 2001, **13**, 308–311.
117 M. Vallet-Regi, F. Balas and D. Arcos, *Angew. Chem., Int. Ed.*, 2007, **46**, 7548–7558.
118 S. Saha, K. C. F. Leung, T. D. Nguyen, J. F. Stoddart and J. I. Zink, *Adv. Funct. Mater.*, 2007, **17**, 685–693.
119 H. Meng, M. Xue, T. Xia, Y.-L. Zhao, F. Tamanoi, J. F. Stoddart, J. I. Zink and A. E. Nel, *J. Am. Chem. Soc.*, 2010, **132**, 12690–12697.
120 J. L. Vivero-Escoto, Slowing II, B. G. Trewyn and V. S. Y. Lin, *Small*, 2010, **6**, 1952–1967.
121 D. P. Ferris, Y.-L. Zhao, N. M. Khashab, H. A. Khatib, J. F. Stoddart and J. I. Zink, *J. Am. Chem. Soc.*, 2009, **131**, 1686–1688.
122 Jie Lu, E. Choi, F. Tamanoi and J.I. Zink, *Small*, 2008, **4**, 421–426.
123 E. Climent, R. Martínez-Máñez, F. Sancenón, M. D. Marcos, J. Soto, A. Maquieira and P. Amorós, *Angew. Chem., Int. Ed.*, 2010, **49**, 7281–7283.
124 A. Schlossbauer, S. Warncke, P. M. E. Gramlich, J. Kecht, A. Manetto, T. Carell and T. Bein, *Angew. Chem., Int. Ed.*, 2010, **49**, 4734–4737.
125 C. Chen, J. Geng, F. Pu, X. Yang, J. Ren and X. Qu, *Angew. Chem., Int. Ed.*, 2011, **50**, 882–886.
126 J. Rosenholm, C. Sahlgren and M. Linden, *J. Mater. Chem.*, 2010, **20**, 2707–2713.
127 K. K. Coti, M. E. Belowich, M. Liong, M. W. Ambrogio, Y. A. Lau, H. A. Khatib, J. I. Zink, N. M. Khashab and J. F. Stoddart, *Nanoscale*, 2009, **1**, 16–39.
128 M. Manzano, M. Colilla and M. Vallet-Regí, *Expert Opin. Drug Delivery*, 2009, **6**, 1383–1400.
129 M. Vallet-Regi, M. Colilla and B. Gonzalez, *Chem. Soc. Rev.*, 2011, **40**, 596–607.
130 H. L. Tu, Y. S. Lin, H. Y. Lin, Y. Hung, L. W. Lo, Y. F. Chen and C. Y. Mou, *Adv. Mater.*, 2009, **21**, 172–177.
131 S. H. Cheng, C. H. Lee, C. S. Yang, F. G. Tseng, C. Y. Mou and L. W. Lo, *J. Mater. Chem.*, 2009, **19**, 1252–1257.
132 D. Brevet, M. Gary-Bobo, L. Raehm, S. Richeter, O. Hocine, K. Amro, B. Loock, P. Couleaud, C. Frochot, A. Morere, P. Maillard, M. Garcia and J. O. Durand, *Chem. Commun.*, 2009, 1475–1477.
133 O. Hocine, M. Gary-Bobo, D. Brevet, M. Maynadier, S. Fontanel, L. Raehm, S. Richeter, B. Loock, P. Couleaud, C. Frochot, C. Charnay, G. Derrien, M. Smaihi, A. Sahmoune, A. Morere, P. Maillard, M. Garcia and J. O. Durand, *Int. J. Pharm.*, 2010, **402**, 221–230.
134 S. H. Cheng, C. H. Lee, M. C. Chen, J. S. Souris, F. G. Tseng, C. S. Yang, C. Y. Mou, C. T. Chen and L. W. Lo, *J. Mater. Chem.*, 2010, **20**, 6149–6157.
135 C. H. Lee, S. H. Cheng, I. P. Huang, J. S. Souris, C. S. Yang, C. Y. Mou and L. W. Lo, *Angew. Chem., Int. Ed.*, 2010, **49**, 8214–8219.
136 J. Gu, S. Su, Y. Li, Q. He, J. Zhong and J. Shi, *J. Phys. Chem. Lett.*, 2010, **1**, 3446–3450.
137 J. M. Rosenholm, E. Peuhu, L. T. Bate-Eya, J. E. Eriksson, C. Sahlgren and M. Lindén, *Small*, 2010, **6**, 1234–1241.
138 C. H. Lee, L. W. Lo, C. Y. Mou and C. S. Yang, *Adv. Funct. Mater.*, 2008, **18**, 3283–3292.
139 J. Lu, M. Liong, Z. X. Li, J. I. Zink and F. Tamanoi, *Small*, 2010, **6**, 1794–1805.
140 A. M. Chen, M. Zhang, D. Wei, D. Stueber, O. Taratula, T. Minko and H. He, *Small*, 2009, **5**, 2673–2677.
141 H. Meng, M. Liong, T. Xia, Z. Li, Z. Ji, J. I. Zink and A. E. Nel, *ACS Nano*, 2010, **4**, 4539–4550.
142 I. P. Huang, S. P. Sun, S. H. Cheng, C. H. Lee, C. Y. Wu, C. S. Yang, L. W. Lo and Y. K. Lai, *Mol. Cancer Ther.*, 2011, **10**, 761–769.
143 Q. J. He, J. L. Shi, M. Zhu, Y. Chen and F. Chen, *Microporous Mesoporous Mater.*, 2010, **131**, 314–320.
144 J. D. Bass, D. Grosso, C. Boissiere, E. Belamie, T. Coradin and C. Sanchez, *Chem. Mater.*, 2007, **19**, 4349–4356.
145 Q. He, Z. Zhang, F. Gao, Y. Li and J. Shi, *Small*, 2011, **7**, 271–280.
146 V. Cauda, A. Schlossbauer and T. Bein, *Microporous Mesoporous Mater.*, 2010, **132**, 60–71.
147 I. Izquierdo-Barba, M. Colilla, M. Manzano and M. Vallet-Regi, *Microporous Mesoporous Mater.*, 2010, **132**, 442–452.
148 Y. S. Lin, N. Abadeer and C. L. Haynes, *Chem. Commun.*, 2011, **47**, 532–534.
149 S. M. Hussain, L. K. Braydich-Stolle, A. M. Schrand, R. C. Murdock, K. O. Yu, D. M. Mattie, J. J. Schlager and M. Terrones, *Adv. Mater.*, 2009, **21**, 1549–1559.

150 T. Laaksonen, H. Santos, H. Vihola, J. Salonen, J. Riikonen, T. Heikkila, L. Peltonen, N. Kurnar, D. Y. Murzin, V. P. Lehto and J. Hirvonent, *Chem. Res. Toxicol.*, 2007, **20**, 1913–1918.
151 M. Fisichella, H. Dabboue, S. Bhattacharyya, M. L. Saboungi, J. P. Salvetat, T. Hevor and M. Guerin, *Toxicol. in Vitro*, 2009, **23**, 697–703.
152 Z. Tao, M. P. Morrow, T. Asefa, K. K. Sharma, C. Duncan, A. Anan, H. S. Penefsky, J. Goodisman and A.-K. Souid, *Nano Lett.*, 2008, **8**, 1517–1526.
153 H. Vallhov, S. Gabrielsson, M. Stromme, A. Scheynius and A. E. Garcia-Bennett, *Nano Lett.*, 2007, **7**, 3576–3582.
154 Y. S. Lin and C. L. Haynes, *Chem. Mater.*, 2009, **21**, 3979–3986.
155 Y. S. Lin and C. L. Haynes, *J. Am. Chem. Soc.*, 2010, **132**, 4834–4842.
156 M. A. Maurer-Jones, Y. S. Lin and C. L. Haynes, *ACS Nano*, 2010, **4**, 3363–3373.
157 D. M. Huang, T. H. Chung, Y. Hung, F. Lu, S. H. Wu, C. Y. Mou, M. Yao and Y. C. Chen, *Toxicol. Appl. Pharmacol.*, 2008, **231**, 208–215.
158 A. J. Di Pasqua, K. K. Sharma, Y. L. Shi, B. B. Toms, W. Ouellette, J. C. Dabrowiak and T. Asefa, *J. Inorg. Biochem.*, 2008, **102**, 1416–1423.
159 Y. Zhao, X. Sun, G. Zhang, B. G. Trewyn, I. I. Slowing and V. S. Y. Lin, *ACS Nano*, 2011, **5**, 1366–1375.
160 A. Nel, T. Xia, L. Madler and N. Li, *Science*, 2006, **311**, 622–627.
161 M. Al Shamsi, M. T. Al Samri, S. Al-Salam, W. Conca, S. Shaban, S. Benedict, S. Tariq, A. V. Biradar, H. S. Penefsky, T. Asefa and A. K. Souid, *Chem. Res. Toxicol.*, 2010, **23**, 1796–1805.
162 W. S. Lin, Y. W. Huang, X. D. Zhou and Y. F. Ma, *Toxicol. Appl. Pharmacol.*, 2006, **217**, 252–259.
163 B. Diaz, C. Sanchez-Espinel, M. Arruebo, J. Faro, E. de Miguel, S. Magadan, C. Yague, R. Fernandez-Pacheco, M. R. Ibarra, J. Santamaria and A. Gonzalez-Fernandez, *Small*, 2008, **4**, 2025–2034.
164 X. L. Huang, J. Zhuang, X. Teng, L. L. Li, D. Chen, X. Y. Yan and F. Q. Tang, *Biomaterials*, 2010, **31**, 6142–6153.
165 S. H. Wu, Y. S. Lin, Y. Hung, Y. H. Chou, Y. H. Hsu, C. Chang and C. Y. Mou, *ChemBioChem*, 2008, **9**, 53–57.
166 T. Liu, L. Li, X. Teng, X. Huang, H. Liu, D. Chen, J. Ren, J. He and F. Tang, *Biomaterials*, 2011, **32**, 1657–1668.
167 S. R. Blumen, K. Cheng, M. E. Ramos-Nino, D. J. Taatjes, D. J. Weiss, C. C. Landry and B. T. Mossman, *Am. J. Respir. Cell Mol. Biol.*, 2006, **36**, 333–342.
168 S. D. Li and L. Huang, *Mol. Pharmaceutics*, 2008, **5**, 496–504.
169 J. S. Souris, C. H. Lee, S. H. Cheng, C. T. Chen, C. S. Yang, J. A. A. Ho, C. Y. Mou and L. W. Lo, *Biomaterials*, 2010, **31**, 5564–5574.
170 A. C. Faure, S. Dufort, V. Josserand, P. Perriat, J. L. Coll, S. Roux and O. Tillement, *Small*, 2009, **5**, 2565–2575.
171 J. H. Park, G. von Maltzahn, E. Ruoslahti, S. N. Bhatia and M. J. Sailor, *Angew. Chem., Int. Ed.*, 2008, **47**, 7284–7288.
172 M. M. van Schooneveld, E. Vucic, R. Koole, Y. Zhou, J. Stocks, D. P. Cormode, C. Y. Tang, R. E. Gordon, K. Nicolay, A. Meijerink, Z. A. Fayad and W. J. M. Mulder, *Nano Lett.*, 2008, **8**, 2517–2525.
173 Q. J. He, J. M. Zhang, J. L. Shi, Z. Y. Zhu, L. X. Zhang, W. B. Bu, L. M. Guo and Y. Chen, *Biomaterials*, 2010, **31**, 1085–1092.
174 E. L. Bentzen, I. D. Tomlinson, J. Mason, P. Gresch, M. R. Warnement, D. Wright, E. Sanders-Bush, R. Blakely and S. J. Rosenthal, *Bioconjugate Chem.*, 2005, **16**, 1488–1494.
175 H. S. Choi, W. Liu, P. Misra, E. Tanaka, J. P. Zimmer, B. I. Ipe, M. G. Bawendi and J. V. Frangioni, *Nat. Biotechnol.*, 2007, **25**, 1165–1170.
176 X. X. He, H. L. Nie, K. M. Wang, W. H. Tan, X. Wu and P. F. Zhang, *Anal. Chem.*, 2008, **80**, 9597–9603.
177 C. Barbe, J. Bartlett, L. G. Kong, K. Finnie, H. Q. Lin, M. Larkin, S. Calleja, A. Bush and G. Calleja, *Adv. Mater.*, 2004, **16**, 1959–1966.